East European Journal of Physics. 4. 250-255 (2024)
DOI:10.26565/2312-4334-2024-4-25 ISSN 2312-4334

INVESTIGATION OF MORPHOLOGICAL AND OPTICAL PROPERTIES OF $LiNbO_3$ AND $LiNbO_3$:Fe 0.03 wt.% CRYSTALS

Murodjon A. Yuldoshev[a]*, Zakirjan T. Azamatov[b], Abror B. Bakhromov[b], Mira R. Bekchanova[c]
[a]*University of business and science, Namangan, Uzbekistan*
[b]*Institute of Semiconductor Physics and Microelectronics, National University of Uzbekistan, 20 Yangi Almazor st., Tashkent, 100057, Uzbekistan*
[c]*University of Public Security of the Republic of Uzbekistan, Tashkent, Uzbekistan*
**Corresponding Author e-mail: murod.yuldoshev1993@gmail.com*
Received October 1, 2024; accepted November 20, 2024

This article is devoted to the morphological and optical properties of the photorefractive crystal $LiNbO_3$ and $LiNbO_3$:Fe 0.03 wt.%. According to it, the surface morphology of the samples was studied using an atomic force microscope (AFM). In addition, ordinary and extraordinary refractive indices of the $LiNbO_3$ crystal were calculated using empirical formulas. The results of the diffraction efficiency of the $LiNbO_3$:Fe 0.03 wt.% crystal for He-Ne and He-Cd lasers are presented.
Keywords: *Lithium niobate; AFM; Holography; Optical absorption*
PACS: 42.40.Eq, 42.40.Lx, 42.70.Mp

INTRODUCTION

Currently, the problem of the most efficient storage of information is particularly acute all over the world [1-4]. One of the effective ways to solve the problem of reliable and long-term storage of information with a high density of information carriers is the holographic method of storing information [1,5,13]. In recent years, comprehensive theoretical and practical research has been carried out in foreign countries to create high-capacity holographic storage devices that record information on various carriers [6-9]. It should be noted that holographic methods make it possible to record, store and restore wave fields, three-dimensional images and other types of information. Lithium niobate crystals, which have a wide band gap, are one of the promising materials used in the field of photonics, quantum electronics, optoelectronics and acoustoelectronics [1,10-13]. Optical properties such as electro-optical, piezoelectric, nonlinear effects, second harmonic generation and refractive index change under laser radiation allow the use of lithium niobate crystals for recording holograms [3,5,14-17].

Holograms created as a result of the photorefractive effect are based on orthogonal nonlinear processes and are also effective for long-wave and high-power lasers. The diffraction efficiency of holograms is practically independent of the intensity of the incident light and can reach 100% in most materials. Therefore, complex detectors and devices were not required. The main disadvantage of coding holograms based on the photorefractive effect is speed. Nonlinear effects become stationary, inversely proportional to intensity. The diffraction efficiency and information transfer rate for the above materials are 1 ms at 1 W/cm^2. However, the low speed of information processing in some materials was not recognized as a disadvantage.

EXPERIMENTAL PART

In holography, two coherent beams are required to form an interference pattern, one called the reference beam and the other called the object beam (the beam scattered from the object). The resulting interference pattern contains information about the amplitude and phase of the object beam. The intensity of the interference pattern can be recorded by placing an appropriate light-sensitive material (such as photographic film or a photorefractive crystal) in the interference region. This recorded fringe pattern or grating is called a hologram. The recorded hologram, when illuminated by the same reference beam, can scatter light in the direction of the object beam. The diffracted beam contains information about the phase and amplitude of the original object beam.

In experiments on studying optical recording in $LiNbO_3$:Fe 0.03 wt.% crystals, we used the scheme shown in Fig. 1.

The data were processed using helium-cadmium (He-Cd, l=440 nm) and helium-neon (He-Ne, l = 630 nm) lasers. The optical sensitivity of the crystal for this wavelength is very high. A virtual interference image in the form of light and dark lines is formed as a result of superradiance of two horizontal waves in the crystal. Double refraction of light occurs in the light lines. That is, a sinusoidal diffraction grating with a period equal to L is observed in the crystal:

$$L = \lambda_{re}[2\sin(\theta_{re}/2)], \quad (1)$$

where, λ_{re} – wavelength of the recording light; θ_{re} – angle between the recording beams. When reading volume holograms ($h \gg \lambda$ and $h \gg L$, where h is the thickness of the hologram) with radiation with a wavelength of λ_r, the angle between the incident and deflected beams is determined by the Wulff-Bragg conditions.

Cite as: M.A. Yuldoshev, Z.T. Azamatov, A.B. Bakhromov, M.R. Bekchanova, East Eur. J. Phys. 4, 250 (2024), https://doi.org/10.26565/2312-4334-2024-4-25

$$2\sin(\theta_r/2) = \lambda_r/\lambda, \quad (2)$$

where, $\theta_r/2$ – angle between the incident beam and the normal to the plate, the angles θ_{re} θ_r are related by the ratio.

$$\sin(\theta_{re}/2)/\sin(\theta_r/2) = {}^{\lambda_{re}}/_{\lambda_r}. \quad (3)$$

The diffraction efficiency of a sinusoidal grating when read by an extraordinary beam with a wavelength is determined by the Kogelnik formula [18]:

$$\eta = \sin^2\{\pi D\Delta n_e/\lambda\cos(\theta/2)\}, \quad (4)$$

where, Δn_e – modulation amplitude of the refractive index of the extraordinary ray, D is the thickness of the crystal, $\theta = \theta_{re}$.

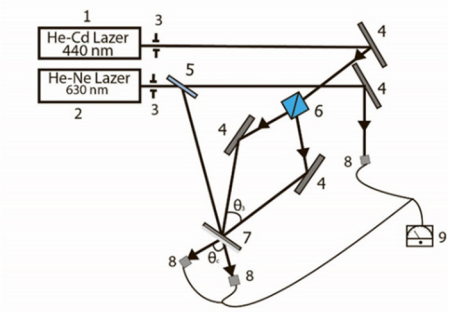

Figure 1. Scheme of the experimental setup: 1- recording laser (He-Cd) λ=440 nm and (He-Ne) λ=630 nm, 2- reading laser (He-Ne) λ = 630 nm, 3-diaphragm, 4-mirrors, 5-light filters, 6-Wollaston prism, 7-$LiNbO_3$:Fe 0.03 wt.% sample, 8-photodetector, 9-microammeter

Experimentally, the diffraction efficiency is defined as the ratio of the intensity of the diffracted reading beam to the intensity of the beam that has passed through the crystal when the hologram is not recorded in the crystal.

These crystals were grown by modified Czochralski grown technique with the use of Donetsk type growth set-up in air atmosphere in a platinum crucible [19].

The samples for research were made from nominally pure and iron-doped $LiNbO_3$ crystals and in the form of parallelepipeds with dimensions of 2×3×10 mm, the edges of which were oriented along the direction of the crystallographic axes. Absorption spectra were studied using a Shimadzu UV 3600 spectrometer. Measurements were carried out in the range of 320-1100 nm with a step of 1 nm. To study the surface morphology of $LiNbO_3$ and $LiNbO_3$:Fe crystals, an NT-MDT atomic force microscope was used. The spectra were processed using the Origin 8.1 software package.

RESULTS AND DISCUSSION

Figure 2 shows the absorption spectra of nominal pure lithium niobate and iron-doped lithium niobate $LiNbO_3$:Fe 0.03 wt.%, from which it is evident that the addition of the impurity significantly increases the absorption.

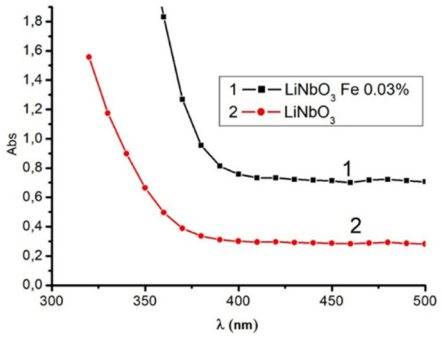

Figure 2. Absorption spectra of iron-doped $LiNbO_3$:Fe 0.03 wt.% and nominally pure lithium niobate

It is known that the use of transition metals as alloying additives is associated with their ability to reversibly donate d-electrons to the conduction band under the influence of radiation.

The resulting absorption spectrum in the decreasing linear part of the graph was approximated by a straight line until it intersected with the abscissa axis. The point where this line intersects the X-axis is the wavelength corresponding to the absorption edge of the crystal. The band gap was determined by the formula:

$$E_g = \frac{hc}{\lambda}, \quad (5)$$

where, λ– wavelength, corresponding to the absorption edge, h – Planck's constant, c – speed of light in vacuum.

One of the main quantities that determine the photorefractive properties of crystals is the refractive index. When determining the band gap width from the absorption spectra, the refractive index of $LiNbO_3$ and $LiNbO_3$:Fe 0.03 wt.% crystals was determined using the following empirical formula proposed by Ghosh [20]:

$$n^2 - 1 = \frac{A}{(E_g+B)^2}, \tag{6}$$

where, $A = 25E_g + 212$, $B = 0.21E_g + 4.25$ and $(E_g + B)$ refer to the corresponding band gap of the material.

The results obtained are respectively: $LiNbO_3$ (E_g=3.39 eV), $LiNbO_3$:Fe 0.03 wt.% (E_g=3,17 eV) and $LiNbO_3$ (n = 2.2922), $LiNbO_3$:Fe 0.03 wt.% (n = 2.3356).

The ordinary and extraordinary refractive indices of the $LiNbO_3$ crystal were calculated using the following formulas in the range λ = 400-5000 nm, the results obtained are presented in the Table.

$$n_o^2 - 1 = \frac{2.9804\lambda^2}{\lambda^2-0.01764} + \frac{1.229\lambda^2}{\lambda^2-0.05914} + \frac{12.614\lambda^2}{\lambda^2-474.6}, \tag{7a}$$

$$n_e^2 - 1 = \frac{2.4272\lambda^2}{\lambda^2-0.02047} + \frac{0.5981\lambda^2}{\lambda^2-0.0666} + \frac{8.9543\lambda^2}{\lambda^2-416.08}. \tag{7b}$$

Table. Ordinary and extraordinary refractive indices of $LiNbO_3$ crystal

λ, μm	**n_e**	**n_o**
0.4	2.191899762	2.509000635
0.5	2.110349304	2.410359464
0.6	2.073558512	2.365369563
0.7	2.052958976	2.340161846
0.8	2.039895099	2.324214431
0.9	2.030848757	2.313219856
1	2.024135933	2.30511079
1.1	2.01885865	2.298783645
1.2	2.014499216	2.293601912
1.3	2.010740815	2.289176022
1.4	2.007380114	2.285255981
1.5	2.004281412	2.281675003
1.6	2.001351109	2.278318112
1.7	1.998522787	2.27510379
1.8	1.995748124	2.271972796
1.9	1.992991166	2.268881124
2	1.990224609	2.265795427
2.1	1.987427319	2.262689961
2.2	1.984582637	2.259544508
2.3	1.981677201	2.256342924
2.4	1.978700112	2.253072109
2.5	1.975642324	2.249721263
2.6	1.972496205	2.246281348
2.7	1.96925521	2.242744676
2.8	1.965913629	2.239104611
2.9	1.962466401	2.235355334
3	1.958908964	2.231491665
3.1	1.95523715	2.227508926
3.2	1.951447084	2.223402828
3.3	1.947535121	2.219169388
3.4	1.943497786	2.214804858
3.5	1.939331726	2.210305664
3.6	1.935033671	2.205668366
3.7	1.930600404	2.200889618
3.8	1.926028732	2.195966131
3.9	1.921315461	2.190894654
4	1.916457381	2.185671942
4.1	1.911451244	2.180294744
4.2	1.906293747	2.17475978
4.3	1.900981523	2.169063724
4.4	1.895511121	2.163203196
4.5	1.889879	2.157174745
4.6	1.88408151	2.150974834
4.7	1.878114889	2.144599835
4.8	1.871975244	2.138046012
4.9	1.865658543	2.131309514
5	1.859160605	2.124386365

The results presented in the table show that the condition $n_o > n_e$ (negative crystal with one optical axis) is fulfilled in all wavelength ranges for the lithium niobate crystal.

The surface morphology of the obtained $LiNbO_3$ and $LiNbO_3$:Fe 0.03 wt.% samples was analyzed using AFM. The size of the study area was (10 mm÷10 mm) (Fig. 3 and 4).

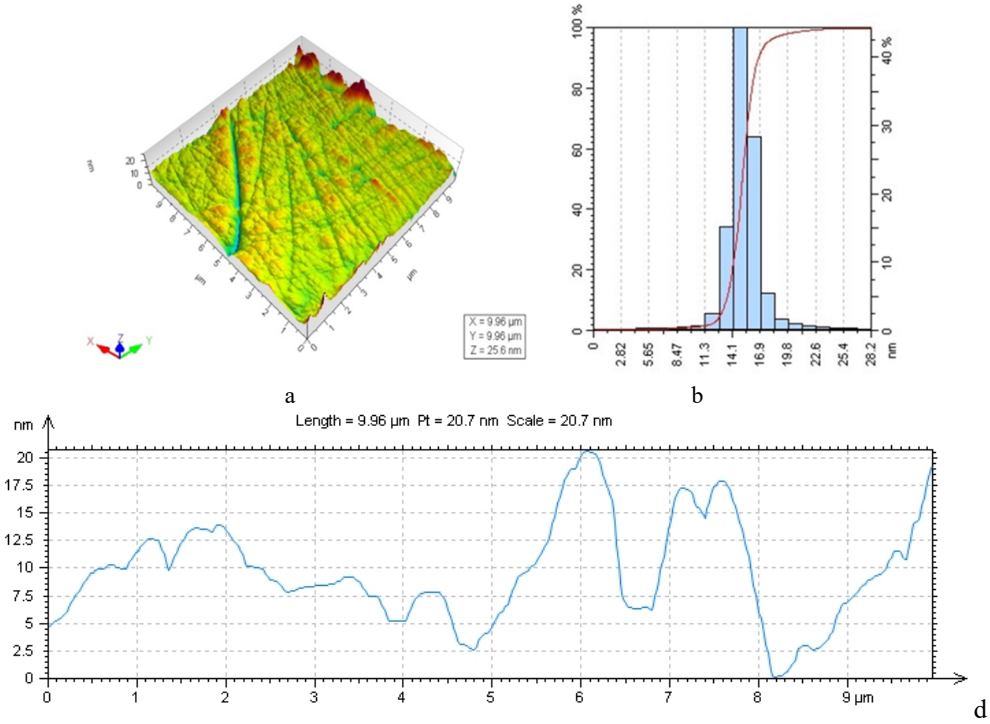

Figure 3. AFM images of the surface morphology of $LiNbO_3$ crystal: a) 3D phase image; b) surface histogram; d) surface relief

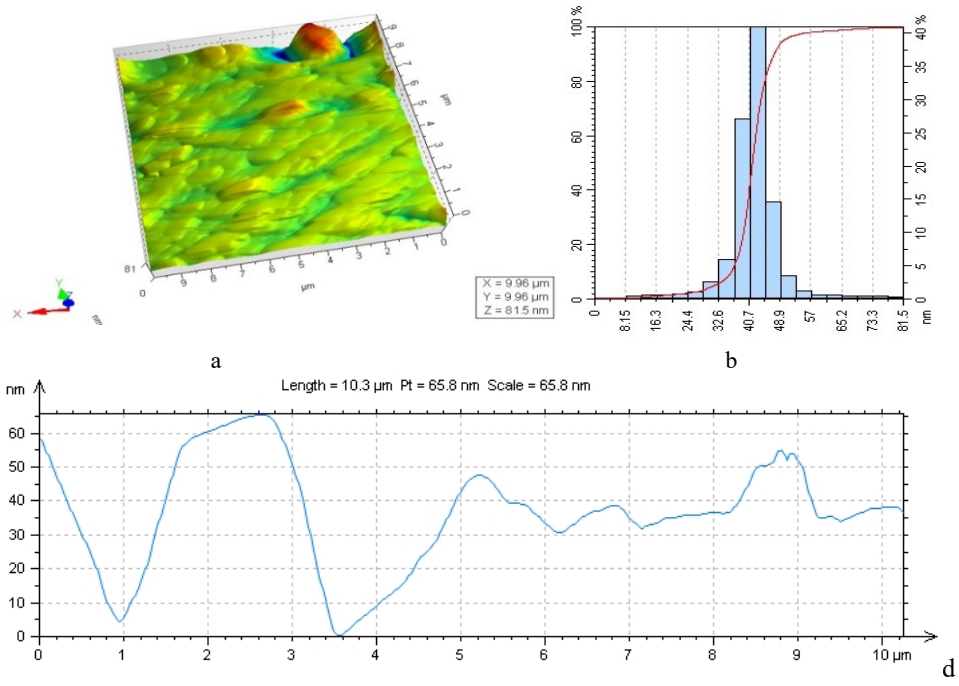

Figure 3. AFM images of the surface morphology of $LiNbO_3$:Fe 0.03 wt.% crystal: a) 3D phase image; b) surface histogram; d) surface relief

The obtained results show that various linear defects were formed on the surface of the $LiNbO_3$ crystal as a result of mechanical treatment (Fig. 3a). This, in turn, affects the distribution and relief of particles on the surface of the sample (Figs. 3b and 3d). The grains formed in the $LiNbO_3$ crystal are in the range (0÷20 nm), and it can be said that most of the surface consists of particles sized 14÷16 nm. In the $LiNbO_3$:Fe 0.03 wt.% samples, the surface morphology is relatively stable, linear defects are practically absent (Fig. 4a). The surface consists mainly of a rounded shape sized 35÷45 nm (Fig. 4b), which means that it is directly related to the influence of iron ions in the structure.

Figure 5 below shows the results of the study of the diffraction efficiency of holograms obtained by He-Ne (l = 630 nm) and He-Cd (l=440 nm) lasers on a $LiNbO_3$:Fe 0.03 wt.% crystal. The results show that the photosensitivity of the crystal increases significantly (2 times) with increasing laser beam power. It is evident that the maximum value of the diffraction efficiency is η=44% for a wavelength of λ=630 nm and η=55% for a wavelength of λ = 440 nm. The fact that the diffraction efficiency reaches a maximum point and then decreases again can be explained by the Chen model [21].

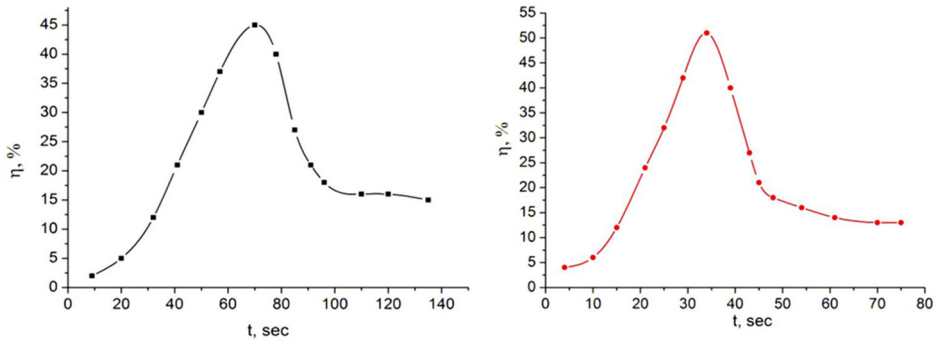

Figure 5. Experimental dependences of the diffraction efficiency of holograms on exposure: a) λ=630 nm; b) λ=440 nm

The interference images of two coherent laser beams are incident on the crystal and recorded as a hologram (Fig. 5). The charge carriers are mainly concentrated in thin layers and are then allowed to move until they recombine with drift and diffusion traps. Thus, the volume and charge are in the same phase as the interference image in the crystal. The electric field of this space charge moves due to the linear electrophoretic effect, and the size of the holographic grating creates the refractive index. Although this procedure depends on first- and second-order electrophoretic effects, it shows that the role of third-order nonlinear effects is significant for the incident beams.

CONCLUSIONS

The studies of photorefractive crystals $LiNbO_3$ and $LiNbO_3$:Fe 0.03 wt.% show that due to iron ions the optical absorption increases significantly (2.5÷3) and the change in the forbidden zone equal to ΔE_g=0.22 eV is established. It was found that the use of expressions 7a and 7b is suitable for the ordinary (n_o) refractive index in the near infrared region and for the extraordinary (n_e) refractive index in the visible and near infrared regions. Morphological analysis shows that iron ions make a significant contribution to the stability of the particle distribution on the surface. Holographically, when using $LiNbO_3$:Fe 0.03 wt.% samples as a memory element and increasing the power of laser beams, it was found that the time to achieve the maximum diffraction efficiency decreased by 2 times.

ORCID

Zakirjan T. Azamatov, https://orcid.org/0000-0001-7074-9437; **Abror B. Bakhromov,** https://orcid.org/0000-0001-8148-2467
Murodjon A. Yuldoshev, https://orcid.org/0000-0002-9722-9439

REFERENCES

[1] V.A. Barachevsky, "The current status of the development of light-sensitive media for holography (a review)," Opt. Spectrosc. **124**, 373–407 (2018). http://dx.doi.org/10.1134/S0030400X18030062
[2] Sh.B. Utamuradova, Z.T. Azamatov, M.A. Yuldoshev, N.N. Bazarbayev, A.B. Bakhromov, East Eur. J. Phys. (4), 147 (2023), https://doi.org/10.26565/2312-4334-2023-4-15
[3] Sh.B. Utamuradova, Z.T. Azamatov, A.I. Popov, M.R. Bekchanova, M.A. Yuldoshev, A.B. Bakhromov, East Eur. J. Phys. (3), 278 (2024), https://doi.org/10.26565/2312-4334-2024-3-27
[4] L. Dai, C. Tan, L. Wang, X. Han, C. Liu, and Y. Xu, "Investigation on nonvolatile holographic storage properties in Hf:Ru:Fe:$LiNbO_3$ crystals as a function of Li composition," Journal of Alloys and Compounds, **753**, 407 (2018). https://doi.org/10.1016/j.jallcom.2018.04.201
[5] T. Volk, M. Wohlecke, "Lithium niobate," in: *Defects, Photorefraction and Ferroelectric Switching*, (Springer, Berlin, 2008).
[6] M.H. Yükselici, D. Bulut, B.C. Ömür, A.A. Bozkurt, and C. Allahverdi, "Optical properties of iron-doped lithium niobate crystal depending on iron content and temperature," Phys. Status Solidi B, **251**, 1265–1269 (2014). http://dx.doi.org/10.1002/pssb.201451071
[7] A.V. Syuy, N.V. Sidorov, M.N. Palatnikov, N.A. Teplyakova, D.S. Shtarev, and N.N. Prokopiv, "Optical properties of lithium niobate crystals," Optik, **156**, 239 (2018). https://doi.org/10.1016/j.ijleo.2017.10.136
[8] N.V. Sidorov, L. A. Bobreva, N. Teplyakova, and G.M. Palatnikov, "Defect Complexes and Optical Properties of Doubly Doped Lithium Niobate Crystals," Inorganic Materials, **54**(10), 1009-1012 (2018). http://dx.doi.org/10.1134/S0020168518100151
[9] E.M. de Miguel Sanz, M. Carrascosa, and L. Arizmendi. "Effect of the oxidation state and hydrogen concentration on the lifetime of thermally fixed holograms in $LiNbO_3$:Fe," Physical Review B, **65**(16), (2002). http://dx.doi.org/10.1103/PhysRevB.65.165101
[10] Sh.B. Utamuradova, Z.T. Azamatov, M.A. Yuldoshev, "Optical Properties of ZnO–$LiNbO_3$ and ZnO–$LiNbO_3$:Fe Structures," Russian Microelectronics, **52**(Suppl. 1), S99-S103 (2023). https://doi.org/110.1134/S106373972360022X
[11] Z.T. Azamatov, M.A. Yuldoshev, N.N. Bazarbayev, and A.B. Bakhromov, Physics AUC, **33**, 139 (2023). https://cis01.central.ucv.ro/pauc/vol/2023_33/13_PAUC_2023_139_145.pdf

[12] Z.T. Azamatov, Sh.B. Utamuradova, M.A. Yuldoshev, and N.N. Bazarbaev. "Some properties of semiconductor-ferroelectric structures," East Eur. J. Phys. (2), 187-190. (2023), https://doi.org/10.26565/2312-4334-2023-2-19
[13] Y.-Y. Li, H.-L. Chen, G.J. Chen, and W.-S. Hwang. "Investigation of the Defect Structure of Congruent and Fe-Doped $LiNbO_3$ Powders Synthesized by the Combustion Method," Materials, **10**(4), 380. (2017). http://dx.doi.org/10.3390/ma10040380
[14] R. Inoue, S. Takahashi, Y. Kitanaka, and T. Oguchi, "Enhanced photovoltaic currents in strained Fe-doped $LiNbO_3$ films," Physica Status Solidi (A) Applications and Materials, **212**(12), (2015). http://dx.doi.org/10.1002/pssa.201532398
[15] Y. Noguchi, R. Inoue, and M. Miyayama, "Electronic Origin of Defect States in Fe-Doped $LiNbO_3$ Ferroelectrics," Advances in Condensed Matter Physics, **2016**(4), 1-10. (2016). http://dx.doi.org/10.1155/2016/2943173
[16] A.S. Pritulenko, A.V. Yatsenko, and S.V. Yevdokimov, "Analysis of the nature of electrical conductivity in nominally undoped $LiNbO_3$ crystals," Crystallogr. Rep. **60**, 267–272 (2015). https://doi.org/10.1134/S1063774515020224
[17] Y.-Y. Li, H.-L. Chen, G.-J. Chen, C.-L. Kuo, P.-H. Hsieh, and W.-S. Hwang, "Investigation of the defect structure of congruent and Fe-doped $LiNbO_3$ powders synthesized by the combustion method," Materials, **10**(4), 380 (2017). https://doi.org/10.3390/ma10040380
[18] H. Kogelik, "Coupled wave theory for thick hologram grating," The Bell System Technical Journal, **48**(9), 2909-2947 (1969). http://users.ntua.gr/eglytsis/IO/Kogelnik_BSTJ_1969.pdf
[19] M.N. Palatnikov, O.V. Makarova, and N.V. Sidorov, "Growth and technological defects in lithium niobate crystals of various chemical compositions," Federal Research Center KSC RAS. pp. 89, (2018).
[20] D.K. Ghosh, L.K. Samanta, and G.C. Bhar, "A simple model for evaluation of refractive indices of some binary and ternary mixed crystals," Infrared Phys. **24**, 43–47 (1984). https://doi.org/10.1016/0020-0891(84)90046-0
[21] F.S. Chen, "Optically induced change of refractive indices in $LiNbO_3$," J. Appl. Phys. **40**, 3389-3393 (1969). https://doi.org/10.1063/1.1658195

ДОСЛІДЖЕННЯ МОРФОЛОГІЧНИХ ТА ОПТИЧНИХ ВЛАСТИВОСТЕЙ КРИСТАЛІВ $LiNbO_3$ ТА $LiNbO_3$:Fe 0,03 мас.%

Муроджон А. Юлдошев[a], Закіржан Т. Азаматов[b], Аброр Б. Бахромов[b], Міра Р. Бекчанова[c]
[a]Університет бізнесу та науки, Наманган, Узбекистан
[b]Інститут фізики напівпровідників та мікроелектроніки Національного університету Узбекистану. Ташкент, Узбекистан
[c]Університет громадської безпеки Республіки Узбекистан, Ташкент, Узбекистан

Дана стаття присвячена морфологічним та оптичним властивостям фоторефрактивного кристала $LiNbO_3$ та $LiNbO_3$:Fe 0,03% мас. Відповідно до нього морфологію поверхні зразків вивчали за допомогою атомно-силового мікроскопа (АСМ). Крім того, за емпіричними формулами розраховано звичайний і надзвичайний показники заломлення кристала $LiNbO_3$. Наведено результати дифракційної ефективності кристала $LiNbO_3$:Fe 0,03 мас.% для He-Ne та He-Cd лазерів.

Ключові слова: *ніобат літію; АСМ; голографія; оптичне поглинання*